Acta Biomaterialia 9 (2013) 5956–5962

Contents lists available at SciVerse ScienceDirect

Acta Biomaterialia

journal homepage: www.elsevier.com/locate/actabiomat

Osteonal lamellae elementary units: Lamellar microstructure, curvature and mechanical properties

Anna Faingold [a], Sidney R. Cohen [b], Natalie Reznikov [c], H. Daniel Wagner [a,*]

[a] Department of Materials and Interfaces, Weizmann Institute of Science, Rehovot 76100, Israel
[b] Chemical Research Support, Weizmann Institute of Science, Rehovot 76100, Israel
[c] Department of Structural Biology, Weizmann Institute of Science, Rehovot 76100, Israel

ARTICLE INFO

Article history:
Received 13 September 2012
Received in revised form 9 November 2012
Accepted 28 November 2012
Available online 6 December 2012

Keywords:
Osteonal lamellae
Fibril orientation
Microstructure
Young's modulus
Nanoindentation

ABSTRACT

The mechanical and structural properties of the sublayers of osteonal lamellae were studied. Young's modulus (E) of adjacent individual lamellae was measured by nanoindentation of parallel slices every 1–3 μm, in planes parallel and perpendicular to the osteon axis (OA). In planes parallel to the OA, the modulus of a lamella could vary significantly between sequential slices. Significant modulus variations were also sometimes found on opposing sides of the osteonal canal for the same lamella. These results are rationalized by considerations involving the microstructural organization of the collagen fibrils in the lamellae. Scanning electron microscope imaging of freeze fractured surfaces revealed that the substructure of a single lamella can vary significantly on the opposing sides of the osteonal axis. Using a serial surface view method, parallel planes were exposed every 8–10 nm using a dual-beam microscope. Analysis of the orientations of fibrils revealed that the structure is rotated plywood like, consisting of unidirectional sublayers of fibrils of several orientations, with occasional randomly oriented sublayers. The dependence of the measured mechanical properties of the lamellae on the indentation location may be explained by the observed structure, as well as by the curvature of the osteonal lamellae through simple geometrical-structural considerations. Mechanical advantages arising from the curved laminate structure are discussed.

1. Introduction

The structure and mechanical properties of osteonal lamellae have been widely investigated on several length scales: starting from the whole osteon [1–5], through several lamellae [6–8] down to the individual lamella [9–16]. In recent years, technological progress has enabled investigation of the microstructural organization of mineralized fibril bundles by X-ray synchrotron beam diffraction [17] and dual ion beam microscopy (FIB-SEM) [18], and through measuring mechanical properties using nanoindentation [16,19] and atomic force microscopy [20,21]. However, the exact organization of those fibrils in osteonal lamellae is still under debate. One theory [22] proposes that the structure is interwoven, with no preferred orientation of fibrils, and with a lamellar structure arising from the alternation of collagen-rich and collagen-poor layers. Another theory states that there is no difference in collagen density in the structure and the fibrils are organized in a rotated plywood-like structure [17,23], comprising five sublayers of parallel oriented fibrils, where each layer is rotated with respect to its adjacent one. However, the most recent studies suggest that neither of these models provides a complete picture, and it is possible that elements of both theories are present [18,24].

Reznikov et al. [18] showed, using the serial surface view method (SSV), that three types of mineralized fibril organizations are present in the circumferential (non-osteonal) lamellae of a rat bone: unidirectional, "fanning" and disordered sublayers. They also claimed that the disordered sublayers were less mineralized than the ordered ones. To date, no study contrasting the osteonal and planar lamellar structures has been reported in the literature. Nevertheless, osteonal lamellae obviously have an additional degree of complexity, being highly curved.

Our recent findings on mechanical properties of individual osteonal lamellae [19] require a more detailed investigation of the structure of those elementary units. In our previous study, Young's modulus (E) of the individual osteonal lamellae was measured by nanoindentation. In the plane parallel to the OA, significant variations of E were observed for single lamellae on opposite sides of the osteon canal. This surprising finding was rationalized in terms of the fibril orientation. The orientation of the exposed mineralized fibrils depends on the cut location (depth) relative to the osteon diameter. In the case of the rotated plywood structure, exposing a diametric cut would reveal fibers with equal orientation on oppo-

* Corresponding author. Tel.: +972 8 934 2594; fax: +972 8 934 4137.
E-mail address: Daniel.Wagner@weizmann.ac.il (H.D. Wagner).

1742-7061/$ - see front matter © 2012 Acta Materialia Inc. Published by Elsevier Ltd. All rights reserved.
http://dx.doi.org/10.1016/j.actbio.2012.11.032

site sides of the canal, assuming the fiber organization has radial symmetry around the canal. In contrast, an eccentric cut would expose fibers with different orientations on the opposite sides of the canal, which should result in different mechanical properties. However, no structural data have been reported to support that explanation.

The objective of the current work is to explore in detail both mechanical and structural properties of the sublayers of osteonal lamellae. This is done by comparing *E* and fiber orientation as functions of depth for individual osteonal lamellae.

2. Experimental

Samples from fresh frozen subchondral part (upper part) of the metacarpal bone of a 5 year old male horse were used. The samples were taken from a site at a distance of about 10–15 cm from the joint. Equine and human osteons are of comparable sizes, being about 200 μm in diameter. The samples were cut using a Minitom cutting instrument (Struers) under constant watering.

2.1. Mechanical properties

A cubic sample with sides of about 0.5 cm was ground and polished manually on planes parallel and perpendicular to the bone axis (“plane 2” and “plane 1”, respectively; see Fig. 1) with SiC papers of grit 360, 800 and 4000, then with diamond powder of 1 and 0.25 μm.

After rinsing, the samples were kept in ambient conditions for at least 24 h (termed here as “dry”) before measurement. After a complete study of the given plane, the sample was finely ground to expose a parallel slice of the same plane (Fig. 2a) and polished to the same grade as the first surface. The fine grinding was performed using 1 μm diamond powder. The width of the removed layer (about 1–3 μm) was monitored by optical microscopy. To avoid confusion, we refer to the slices produced by grinding and polishing as “p-slices”.

Nanoindentation measurements and topographical scans were performed with an XP-Nanoindenter (Agilent) equipped with a Berkovich tip. Topographical scanning was performed at a constant force of 1.4 μN (for details see [19]). The indentations were made by loading the sample at a constant strain rate of 0.05 s^{-1} until a maximum displacement of 180 nm was reached, which required a loading force of about 400–500 μN. *E* was calculated using the Oliver and Pharr method [25]. All nanoindentation measurements were performed in continuous stiffness measurement (CSM) mode, for which a 2 nm harmonic modulation is superimposed on the loading curve at a frequency of 75 Hz. Modulus and hardness values are then obtained continuously during the loading segment. The CSM mode is particularly useful for nanomechanical studies on nonuniform samples such as bone and teeth [26]. Full details of the procedure used here are described elsewhere [19]. Imprints of up to 1.3 μm lateral length could be observed by post-indent images made with the indenter tip and the Nanovision™ module of the nanoindenter.

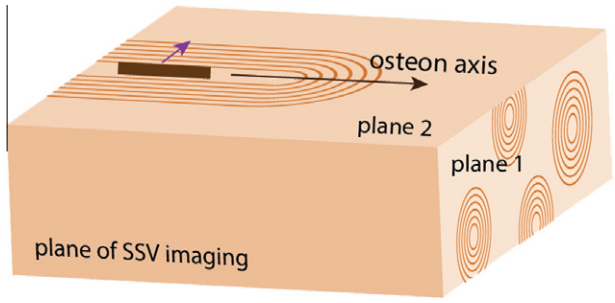

Fig. 1. Schematic illustration of an osteonal bone sample indicating the osteon axis (black arrow) and the planes of interest: plane 1 (perpendicular to OA), plane 2 (parallel to OA) and the SSV imaging plane. SSV imaging starts at the location marked by the rectangle and propagates in the direction of the adjacent arrow (parallel to plane 1).

All nanoindentation measurements were performed on thick lamellae only (Fig. 2b). The thin lamellae could not be measured as their thickness (no more than 1 μm) was comparable to the indent lateral size. Thus, measurements would not be confined to the lamella borders and edge effects would render the results unreliable. From here on, “lamella” refers to the thick lamellae only, unless otherwise specified.

Indentations of the osteons were made in the four lamellae closest to the Haversian canal. The same lamellae on the opposite sides of the canal were tested (Fig. 2a), with 8–15 indentations in each lamella on each side.

Nine osteons were studied in plane 2 at 2–5 depths, as defined by parallel slicing (p-slices) and shown in Fig. 2. For comparison, three osteons in plane 1 were studied, at three different depths each.

To compare lamellar properties on opposite sides of the canal or between the p-slices, a Student’s *t*-test was performed with a significance level of 0.05.

2.2. Mineralized fibrils microstructure

2.2.1. Scanning electron microscopy (SEM)

Thin specimens (about 20 mm × 5 mm × 1 mm) were cooled in liquid nitrogen for 30 min and then fractured, exposing a random surface in plane 2. In this way, a brittle fracture of the surface is achieved, minimizing plastic deformation during fracture and thus preserving the natural orientation of fibril bundles. The long dimension of the sample was selected to be parallel to plane 1, thereby simultaneously exposing both sides of the osteonal canal as the crack propagated, to ensure that the fracture propagates along the osteon axis (rather than perpendicular to it).

Fractured surfaces were subsequently coated with gold–palladium to prevent charging and observed in a SUPRA 55 (Zeiss) scanning electron microscope at 3 kV. All images were taken using the secondary electrons (SE) detector.

2.2.2. Serial surface view

2.2.2.1. Demineralization and staining. Samples of about 30 mm × 30 mm × 0.2 mm were ground and polished following the same procedure as for the mechanical studies, exposing plane 2. Next, the samples were demineralized by immersion in a solution of 5% ethylenediaminetetraacetic acid (EDTA) and 2% paraformaldehyde in cacodylate buffer, pH 7, for 48 h on a rocking table. After demineralization, residual EDTA was washed using deionized water (DW) in three steps (twice for 4 h, then once for 12 h) while agitating on a rocking table. Then the samples were fixed again with 4% gluteraldehyde in cacodylate buffer (pH 7) overnight and washed with DW in the three steps mentioned earlier. The staining was performed using the OTOTO protocol, whereby osmium tetroxide (O) and thiocarbohydrazide (T) are applied sequentially, following the procedural steps described by Reznikov et al. [18]. Finally, the sample was kept in ambient conditions for at least 24 h.

2.2.2.2. Imaging. A Helios Nanolab 600 (FEI™) FIB-SEM was used for the SSV. The sample was elevated to the eucentric height (the height where the sample can be tilted without changing its height on the optical axis and remain in focus) and tilted to 52° so that the electron beam and the ion beam were focused on the same point. An osteonal canal was identified at low magnification and was set to permit the SSV to start as close as possible to the canal and to proceed into the lamellar structure (Fig. 1). However, the fibrillar pattern is not visible at the surface of the first lamella inside the